Enhancement on Energy Extraction from Magnetic Energy Harvesters

Jinyeong Moon, Steven B. Leeb
Department of Electrical Engineering and Computer Science
Massachusetts Institute of Technology
Cambridge, MA 02139, USA

***Abstract*—This paper presents a method for enhancing performance of a magnetic energy harvester. The harvester operates with a magnetically saturating core with high magnetic permeability. If the core saturates, the effective magnetizing inductance becomes small, and little power can be harvested from the core. Energy is harvested very efficiently during an operating cycle when the core is not saturated, a time period we call the "transfer window." It can be shown that the location and the length of a transfer window are independent of each other. Based on this property, the transfer window alignment (TWA) method is introduced for maximizing power harvest. The TWA method manipulates the location of the time window, and harvests a greater amount of power compared to passive rectification. The principle of the TWA method reveals that deeper core saturation with higher voltage stress leads to a higher level of energy extraction. The analysis of the TWA method is presented, and verified with simulation and experiments. A detailed control sequence for actual implementation is presented. The TWA method poses little burden to hardware complexity.**

***Index Terms*—Transfer window alignment, magnetic energy, energy harvesting, magnetic saturation**

I. Introduction

Self-powered sensor nodes are extremely useful in monitoring applications [1], [2], [3], [4], where battery maintenance or custom sensor power wiring are challenges. By harvesting energy from magnetic fields generated by the current flowing around a convenient power line used for other equipment such as a motor, a magnetic energy harvester can extract a relatively high amount of energy per volume (or size), compared to other energy harvesting methods, such as vibration [8], [9], temperature [10], radio waves [11], etc [4]. The amount of energy that can be extracted by a magnetic energy harvester is rarely affected by ambient conditions as long as the equipment to be monitored is carrying the current. This distinguishes the magnetic approach from photovoltaic sources or other environmental sources like vibration or wind.

This paper introduces the "transfer window alignment (TWA)" algorithm to enhance energy extraction from a magnetic energy harvester. This method boosts the amount of energy extracted in comparison to passive rectification. A conceptual model is explored first, followed by a description of the proposed control implementation. The TWA method reduces overall semiconductor count in the harvester by taking advantage of microprocessor control of active rectifiers.

With the proposed method, a magnetic energy harvester can extract approximately $12\,\mathrm{mW}$ per every $1\,\mathrm{A_{RMS}}$ of primary side current with an amorphous nanocrystalline magnetic core as small as $2.9\,\mathrm{cm}^3$. To get a first cut of power per surface area comparison, assume a primary device that operates with $10\,\mathrm{A_{RMS}}$, which is a reasonable range for a line frequency device, and a depth of a magnetic core of $1\,\mathrm{cm}$, which is comparable to the thickness of casings in 2-D technologies, such as temperature and vibration energy harvesting. For comparison, our magnetic energy harvester extracts approximately $120\,\mathrm{mW}$ with a surface area of $2.9\,\mathrm{cm}^2$; on the other hand, temperature energy harvesting would require $1200\,\mathrm{cm}^2$ [10] (assuming $\Delta T = 10\,\mathrm{K}$), and vibration energy harvesting would require $600\,\mathrm{cm}^2$ [4]. These alternatives generally require larger surface area to provide similar levels of energy extraction. Furthermore, even though solar ($15\,\mathrm{mW/cm}^2$ [4]) and wind ($1200\,\mathrm{mW\,h/day}$ [4]) energy harvesting can extract a substantial amount of energy, they cannot be used in small and confined (dark) spaces, e.g., inside of a motor's control box for diagnostic sensing.

II. Background

A. Magnetic Energy Harvesting

The approach to magnetic energy harvesting described in this paper employs a periodically and magnetically saturating core. The energy is harvested purely from magnetic fields generated by an AC current that flows through a primary device to be monitored without any permanent magnet or vibration associated. The core (Vitroperm 500F W380 by VAC) is an amorphous nanocrystalline core with very high initial magnetic permeability. A nanocrystalline core is beneficial in that it has a relatively high magnetic saturation flux density, and exhibits a very low hysteresis loss, making mW range power harvesting feasible. Its very high magnetic permeability ensures development of a sufficient voltage across the core to allow a rectifier to transfer power to a load when the core is not saturated. Other core types, for example, powdered iron or ferrite cores, have difficulties in developing a sufficient voltage across the core to overcome the voltage set by a rectifier and a load for power transfer because of relatively low magnetic permeabilities. As seen in [1], a relative magnetic permeability has to be at least on the order of hundreds of thousands, which is hardly achievable using any powdered or ferrite core.

As opposed to conventional transformers or inductors, a core in a magnetic energy harvester is intentionally put into magnetic saturation in every half line cycle. This is because

978-1-4673-7151-3/15/$31.00

magnetic saturation is essential for maximum energy extraction in passive rectification as introduced in [6] and in the TWA method as will be discussed later in this paper. A primary side with a single winding is coupled with a secondary side with hundreds of turns, much like a conventional current transformer except for that magnetic saturation is heavily exploited here. The B-H curve of a core material and Maxwell's equations as well as the external circuit constraints determine when magnetic saturation occurs and when the core is restored from saturation. For accurate analyses, a numerical simulator is built in [6] to compute very nonlinear responses of this system. However, in this paper, first order approximations will be used for a qualitative analysis and design directions in the expense of accuracy.

B. Rectifier and Load

Understanding the magnetic core as a nonlinear AC current source, harvested magnetic energy is implied by a generated electric current. However, the energy can be "harvested" when the generated current is subject to a voltage potential, for example, a supercapacitor charged to a certain voltage level. If there is zero voltage potential across the two terminals of the core (shorted core), all the generated current in the secondary side goes back to the primary side through the transformer, harvesting zero power. To store the energy as charge (hence as voltage), a capacitor — supercapacitor for greater energy density — is used as a load for the core, and a rectifier is required to eliminate bilateral signs of the transformer current before joining the capacitor with the core. The supercapacitor will be the direct source of electric energy for subsequent circuit blocks. A voltage regulator will be used to provide a stable voltage reference to the rest of the circuits, controlling current inflow from the core and current outflow to the circuit. In the viewpoint of line frequency, which is 50 to $60\,\mathrm{Hz}$, a supercapacitor with a mF to F range can be considered as a constant voltage load in the scope of a half line cycle time and a primary current up to hundreds of ampere. Therefore in the analysis, the load capacitor will be represented by a constant load voltage, V_{LOAD}. Two supercapacitors (PAS0815LS2R5105 by Taiyo Yuden) are connected in series to allow a maximum voltage rating of $5\,\mathrm{V}$ with capacitance of $0.5\,\mathrm{F}$. The effective series resistance (ESR) of two supercapacitors in series is approximately $140\,\mathrm{m\Omega}$.

C. Core Saturation and Transfer Window

Once a magnetic core is saturated, an operating point on a B-H curve is at a "flat tail" side, making $\partial B/\partial t$ close to zero. It is not perfectly zero as the permeability of air still exists, but it is negligible for coupling harvested energy. Since the time derivative of B is directly proportional to the voltage developed across the core terminals, the voltage (hence impedance) across the two terminals of the core is essentially zero. Therefore, as long as the core is saturated, no power (or energy) can be harvested from the core. On the other hand, when a magnetic core is yet to enter saturation, a very high magnetic permeability and low hysteresis loss of an amorphous nanocrystalline core result in a very high shunt inductance, and the core essentially serves as a very efficient current source, transferring the entire transformer current to a load until saturation. This partially helps illuminate why core saturation maximizes energy extraction in magnetic energy harvesting with passive rectification: if a core is not saturated, a higher load voltage can be applied until it causes saturation, and since the core serves as a near-ideal current source until then, the power harvest directly increases as the load voltage increases.

A time window during which a core serves as a near-ideal current source in each half cycle is termed a "transfer window." This is equivalent to the duration which the core is not saturated for. For a magnetic core with an ideal diode rectifier, a transfer window starts at a zero crossing of a transformer current, assuming very low hysteresis loss, and ends at when the core is saturated for the first time in the half cycle. A way to estimate the length of a transfer window in the first order will be shown in the next section.

III. Improving the Energy Extraction - Transfer Window Alignment

In [6], background and theoretical analysis of a pure magnetic energy harvester is presented in detail, where the rectifier in the analysis is assumed to be a full bridge diode rectifier with either ideal diodes or FETs to mimic ideal diodes once a current path is decided. This can effectively decrease the conduction loss due to diode voltage drop. However, it still means that the operation of energy harvesting relies on the passive response of the rectifier driven by the primary current, referencing to zero crossings of the primary current. Though the accurate response must be calculated using the numerical method given in [6], the first order hand approximation can be helpful to explore the limit of passive rectification. Referenced to the time point with zero primary side current, $t = t_0$, where the core must be certainly out of magnetic saturation, the cyclic average power can be written as follows:

$$P_{\mathrm{avg}} = \frac{2}{T}\int_{t_0}^{t_0+t_{\mathrm{SAT}}} \frac{I_{\mathrm{P}}}{N}\sin(\omega\,(t-t_0))\cdot V_{\mathrm{LOAD}}\;\mathrm{d}t \qquad (1)$$

Here, T, I_{P}, N, ω, and V_{LOAD} denote the period of the primary side sinusoid, the peak amplitude of the primary side current, the number of windings in the harvester side, the angular frequency of the primary side, and the voltage of the supercapacitor, respectively. Note that the power is averaged over a half cycle because of the rectification. Also, t_{SAT} indicates the length of a transfer window — the amount of time that is needed to saturate the core from the zero current state with given environmental parameters. The constant voltage load is assumed to represent a supercapacitor as an energy storage. This equation states that the primary current is reflected to the secondary side with an $N:1$ ratio, and delivers the full current to the supercapacitor until the core goes into saturation. Practically, a numerical solver is required to predict the accurate amount of harvested power, as stated in [6], because a calculation of t_{SAT} involves a nonlinear B-H curve of a core material combined with a differential equation

TABLE I
CORE PARAMETERS - VAC 500F W380

B_{SAT}	1.190 T
$P_{\mathrm{LOSS\text{-}MAX}}$	0.125 mW
α	2.2
Outer Radius (r_{OD})	12.25 mm
Inner Radius (r_{ID})	8.25 mm
Height (h)	9 mm
Flux Area (A_{CORE})	3.6×10^{-5} m^2

imposed by Maxwell's equations. There is also a nonconstant voltage developed across the supercapacitor due to the effective series resistance. However, in the first order, an approximation using the flux balance can be used to find t_{SAT}:

$$V_{\mathrm{LOAD}} \cdot t_{\mathrm{SAT}} = 2 \cdot B_{\mathrm{SAT}} \cdot A_{\mathrm{CORE}} \cdot N \tag{2}$$

The coefficient '2' in (2) accounts for the full swing of B field, from $-B_{\mathrm{SAT}}$ to $+B_{\mathrm{SAT}}$ in a half cycle if the core indeed experiences magnetic saturation. Considering (2), it is evident that t_{SAT} does not depend on the primary side information in the first order. This indicates that the core goes into saturation as soon as V_{LOAD} is connected to the core for a duration equal to or longer than t_{SAT}. A critical finding is that changing a starting point of such connection does not affect the calculation of the length of t_{SAT} — in the same sense, even the number of such connections within a half cycle can be multiple as long as the total length of t_{SAT} stays the same. Therefore, the integration range of equation (1) can be freely modified without affecting t_{SAT} in the first order. In short, t_{SAT} is governed by (2), which is almost a physical constant, and the time window where the core is not saturated can be freely shifted.

The best strategy is to shift the transfer window, so that the middle of the transfer window is aligned with the peak of the primary current. Since the primary side is sinusoidal, the transfer window will be recurring every half cycle, and symmetric around the quarter wave length point of the primary side current. The effect of aligning the transfer window can be easily verified through the simulation result given in Fig. 1. The parameters of the magnetic core that is used throughout this paper are summarized in Table. I. Note that $P_{\mathrm{LOSS-MAX}}$ and α are calculated as defined in [6]. The solid curve without any mark indicates the secondary side transformer current, an $N:1$ reflection of the primary side current. The curve marked with 'x' indicates the case for ideal passive rectification. The curve marked with dot indicates the case with the transfer window alignment (TWA) method. The transfer window of the TWA method has been clearly shifted to align its midpoint with the peak of the primary current whereas the transfer window of the passive rectification case starts as soon as the transformer current crosses zero. As discussed, the lengths of the transfer window in both cases stay almost constant. Since the amount of harvested energy is directly proportional to the average harvested current multiplied by the supercapacitor voltage,

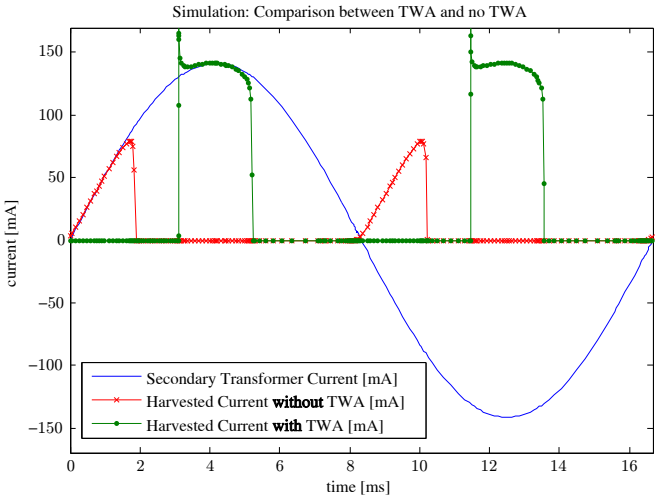

Fig. 1. The effect of the TWA method

which is assumed constant, the boost in the energy extraction can be easily seen by comparing the levels of the currents in both cases in the figure. In this simulation with $I_{\mathrm{P}} = 10\,\mathrm{A_{RMS}}$, $N = 100$, and $V_{\mathrm{LOAD}} = 4\,\mathrm{V}$, the TWA method harvests 139.1 mW whereas the passive rectification harvests 41.3 mW. Also, the difference between the amount of energy extractions using the TWA method and passive rectification will grow as the core goes into deeper magnetic saturation, because the average current of passive rectification will continually go down in heavier saturation while the average current of the TWA method will converge to the peak of the sinusoid.

In order to analyze when the maximum energy extraction occurs with the TWA method, the following approximated expressions for the average power delivery can be derived:

$$\begin{aligned} P_{\mathrm{avg}} &= \frac{2}{T} \int_{\frac{T}{4}-\frac{t_{\mathrm{SAT}}}{2}}^{\frac{T}{4}+\frac{t_{\mathrm{SAT}}}{2}} \frac{I_{\mathrm{P}}}{N} \sin(\omega t) \cdot V_{\mathrm{LOAD}}\, \mathrm{d}t \\ &= \frac{2\, I_{\mathrm{P}}}{\pi\, N} \cdot V_{\mathrm{LOAD}} \cdot \sin\left(\frac{\omega\, t_{\mathrm{SAT}}}{2}\right) \\ &= P_{\mathrm{TWA}} \cdot \frac{\sin(J)}{J} \end{aligned} \tag{3}$$

Here, P_{TWA} represents an asymptotic maximum. It is defined as:

$$P_{\mathrm{TWA}} = \frac{2\, I_{\mathrm{P}}\, \omega\, B_{\mathrm{SAT}}\, A_{\mathrm{CORE}}}{\pi} \tag{4}$$

J is a design variable, proportional to t_{SAT}. It is defined as:

$$J = \frac{\omega\, B_{\mathrm{SAT}}\, A_{\mathrm{CORE}}\, N}{V_{\mathrm{LOAD}}} = \frac{\omega\, t_{\mathrm{SAT}}}{2} \tag{5}$$

Examining (3), the amount of power harvest has the asymptotic maximum of P_{TWA} as $J \to 0$. So, in order to maximize the energy extraction, J should be minimized as much as possible, which also directly shortens t_{SAT} as stated in (5). This finding indicates that the maximum energy extraction happens when the core is driven to extreme saturation with

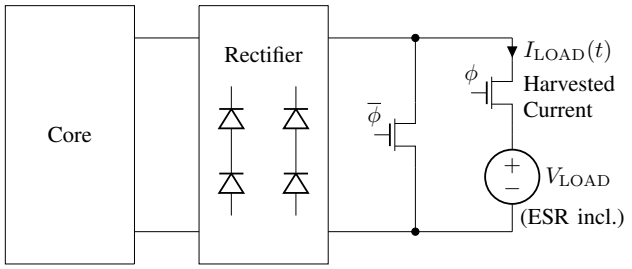

Fig. 2. Conceptual implementation of the TWA method

an infinitely small transfer window with an infinitely high load voltage level. This is also consistent to the explanation of the average current converging to the peak value of the sinusoid. However, such infinitely small J (hence infinitely small t_{SAT} too) is to be avoided because 1) the first order approximation is violated in the extreme region, and 2) it is impractical. Nonetheless, in a nonextreme saturation region, an interesting point still holds true: the energy extraction increases as the core goes into deeper saturation. This is a direct opposite to the usage of conventional transformers or inductors, which are operated in a non-saturation region only. Based on our experimentation with high permeability cores at utility line frequencies, a practical suggestion is to select $t_{\mathrm{SAT}} \geq \frac{T}{10}$, in which case $J \geq 0.314$. With $J = 0.314$, the amount of energy extraction is 98.36% of the asymptotic maximum P_{TWA}. However, such a low value of J can sometimes impose an impossible circuit constraint, for example, V_{LOAD} being too high compared to a voltage rating of a supercapacitor or N being too low for windings to allow high secondary current. Therefore, a trade-off between voltage/winding constraints and energy extraction must be carefully considered.

Conceptual implementation of this method is illustrated in Fig. 2 with two additional FETs outside the rectifier. The operation of Fig. 2 is simple. It is either 1) shorting out the rectifier to delay the transfer window or 2) providing a regular current path as a normal rectifier does when energy extraction is supposed to occur. When the rectifier is shorted, the voltage across the core is forced to be zero, rendering zero flux accumulation for the core toward magnetic saturation. On the other hand, when the transfer window is initiated, the core sees a constant voltage of the supercapacitor, and steadily accumulates flux, eventually leading to magnetic saturation. Note that since the positive terminal of the supercapacitor cannot be shorted to ground at any point, the gate controls (ϕ and $\overline{\phi}$) for two added FETs must be carefully timed so that both FETs cannot conduct at the same time. Even so, however, a realistic circuit should not be built based on Fig. 2 because shorting out the rectifier does not always guarantee close-to-zero impedance (or voltage) across the magnetic core. For example, if the rectifier is a full bridge diode rectifier, shorting out the rectifier still exhibits $2\,V_{\mathrm{DIODE}}$ across the core whenever the secondary current is present, where V_{DIODE} refers to diode voltage drop. So, the core continuously accumulates volt-second

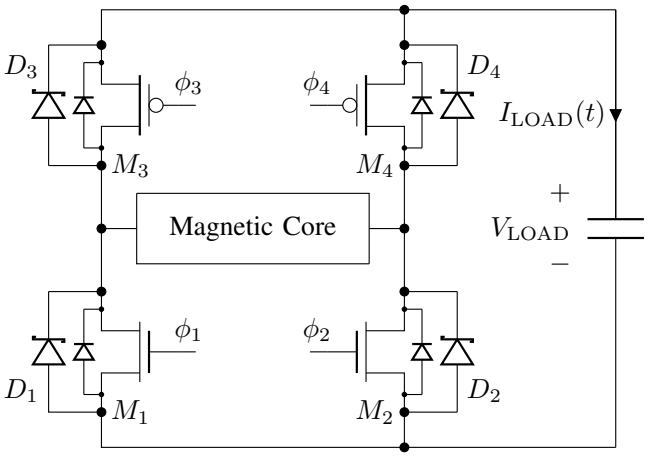

Fig. 3. Actual implementation of the TWA Method

(flux) even when it is supposed to be shorted. It obviously results in faster magnetic saturation, lowering power harvest. As an example, the amount of power harvest with the TWA method is estimated with $I_{\mathrm{P}} = 10\,\mathrm{A_{RMS}}$, $N = 100$, $V_{\mathrm{LOAD}} = 4\,\mathrm{V}$, and $V_{\mathrm{DIODE}} = 0.3\,\mathrm{V}$ (assuming Schottky diodes). Other than the diode voltage drop, the circuit parameters are identical to the parameters used in Fig. 1. The TWA method gives $139.1\,\mathrm{mW}$ if the core is perfectly shorted while delaying the transfer window, and $85.9\,\mathrm{mW}$ if there are two real diodes in the current path while delaying the transfer window. Even though the TWA method with realistic diodes is superior to the passive rectification only ($41.3\,\mathrm{mW}$), a substantial amount of energy is lost due to nonideal flux accumulation during when the core is supposed to be shorted. In order to completely eliminate this issue, the TWA method requires full knowledge of the rectifier performance.

A better implementation is proposed in Fig. 3. This circuitry is identical to the general active rectifier, with the additional benefit that two additional FETs for TWA operations in Fig. 2 have been eliminated. Note that a rectifier in a magnetic energy harvester, which is essentially a nonlinear current transformer, does not suffer from a dead time near zero crossings of a sinusoid unlike a rectifier in a voltage transformer does. This stays true regardless of a type of a rectifier, for example, a diode rectifier. The operations of the TWA method is now implied by the control method, and incorporated with active rectification. The control signals and important time points that separate the operation regions are labeled in Fig. 4.

Region 1 ($t_0 \leq t < t_1$): this region is used to detect a zero crossing of a transformer current, using diodes only. Since a magnetic energy harvester works as a current transformer, as soon as the current conducts, either the left or the right node of the magnetic core will exhibit the full load voltage. A microcontroller will monitor the voltage of both sides to detect a zero crossing of the current. In this phase, ϕ_1 and

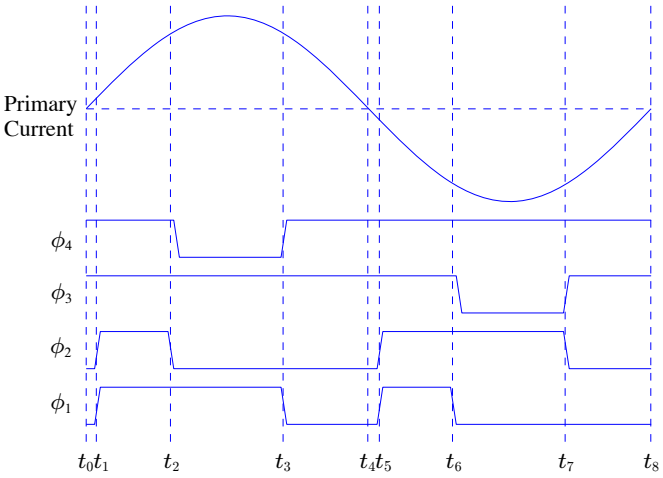

Fig. 4. Control signals and operation regions of the TWA Method

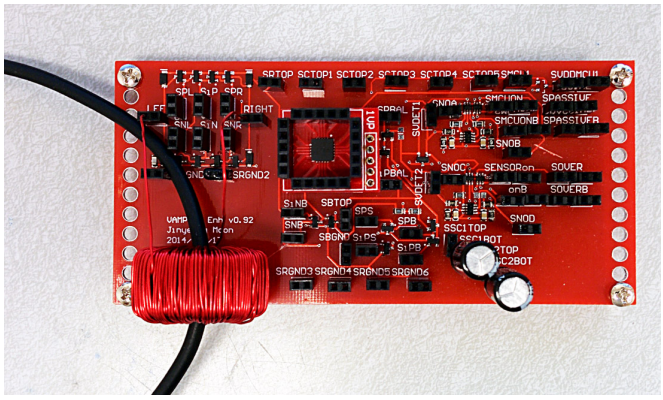

Fig. 5. Test circuit board

ϕ_2 are driven low to switch off NFETs, and ϕ_3 and ϕ_4 are driven high to switch off PFETs. A zero crossing detection is performed every cycle to continuously synchronize a microcontroller with the line frequency so that the location of the transfer window can be accurately estimated every cycle without dedicated training cycles that will periodically stall the microcontroller. The diagram exaggerates the length of this region for a clearer illustration.

Region 2 ($t_1 \leq t < t_2$): as soon as the zero crossing is detected, the length of the previous cycle period can be obtained by comparing the timestamp of the current zero crossing to the timestamp of the previous zero crossing. The microcontroller uses the information of the most recent zero crossing, the length of the previous cycle period, and the length of the previous transfer window for estimating the location of the current transfer window. As soon as all the required timing calculations for the upcoming transfer window are done, both NFETs are driven high to short out the core. A negligible amount of flux will be accumulated for the magnetic core during this phase. PFETs are still driven high to make sure that the supercapacitor is isolated from the grounded core. The core is intentionally shorted to delay the transfer window.

Region 3 ($t_2 \leq t < t_3$): one of the NFETs is now turned off to move the core out of the shorted state. For example, ϕ_2 is driven low in Fig. 4, intending a current flow with M_1 and M_4. However, the control for M_4 that will drive ϕ_4 low cannot take place at the same time as ϕ_2 transitions to low to avoid a short-circuiting path of the supercapacitor, similar to the ϕ and $\overline{\phi}$ control in Fig. 2. In order to reflect this, ϕ_4 in Fig. 4 is driven low slightly after ϕ_2 makes the transition. This phase is where the most of the energy extraction occurs. The transfer window is initiated, shifted from the zero crossing of the sinusoid, and the maximum current over a window that is t_{SAT} long is extracted from the core through the active rectifier. This phase ends when the core goes into saturation, and the microcontroller records such an event so that the information can be used to estimate the location of the transfer window in the next cycle.

Region 4 ($t_3 \leq t < t_4$): as soon as the core goes into saturation, all the FETs are switched off. Only diodes are used to commutate the direction of the current in the rectifier. This prepares the detection of the next zero crossing of the transformer current.

Region 5 ($t_4 \leq t < t_5$): this serves the same purpose as the region 1, except for that the current direction is now reversed. Therefore, a zero crossing will be detected on the other side of the core.

Region 6 ($t_5 \leq t < t_6$): this serves the same purpose as the region 2.

Region 7 ($t_6 \leq t < t_7$): this serves the same purpose as the region 3, except for that the current is supported by M_2 and M_3. Note that ϕ_3 also transitions slightly after ϕ_1 is driven low to avoid a short-circuiting path of the supercapacitor.

Region 8 ($t_7 \leq t < t_8$): this serves the same purpose as the region 4.

With this implementation, not only the number of switches are lower, but also the core never accumulates unwanted flux when it is intentionally shorted, except for volt-second developed by the intrinsic on-resistance of the FETs and DC wire resistance. The cross-coupled FETs, discussed in [7] to reduce the control efforts, unfortunately cannot be used in one of the top or bottom slots in the rectifier anymore, because it will present a short-circuiting path for the supercapacitor during the intentional short-out period of the core. However, the voltage regulation switches in [7] can be integrated into active rectification as well, much like the two TWA switches are integrated into Fig. 3 in the expense of additional control efforts in active rectification.

IV. Experimental Results

The test circuit board is presented in Fig. 5. The scopeshot of the TWA method and active rectification is given in Fig. 6. A heater, which consumes $5.5\,\mathrm{A_{RMS}}$, was used as a primary

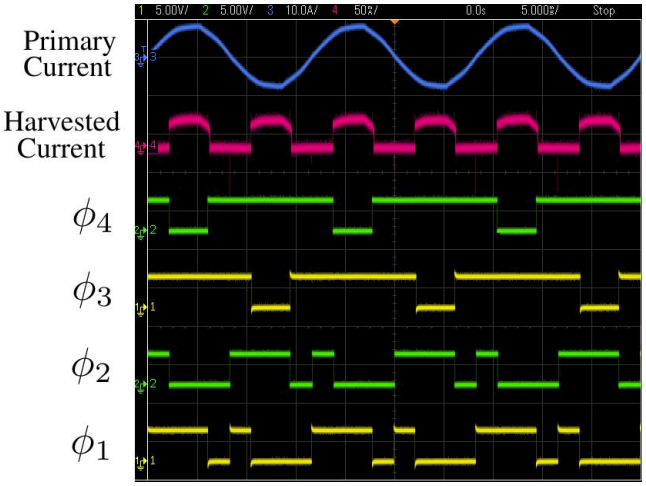

Fig. 6. Oscilloscope screenshot of the TWA method and active rectification

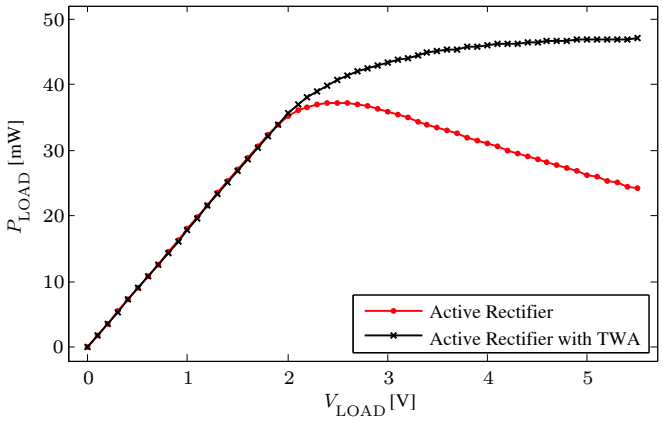

Fig. 7. Power harvest vs. level of core saturation with the TWA method

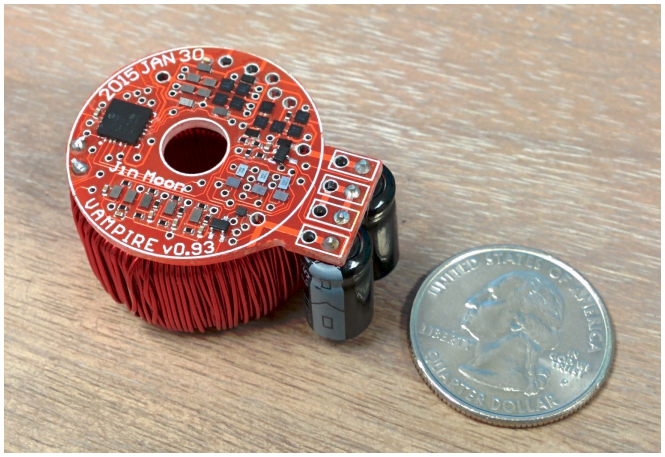

Fig. 8. Magnetic energy harvester prototype including the TWA method

side. The harvested power is 65.9 mW ($I_{\mathrm{LOAD,avg}} = 16.30\,\mathrm{mA}$ at $V_{\mathrm{LOAD}} = 4.04\,\mathrm{V}$) with $N = 200$. Using identical settings except for the rectifier, passive rectification harvests 38.6 mW ($I_{\mathrm{LOAD,avg}} = 9.65\,\mathrm{mA}$ at $V_{\mathrm{LOAD}} = 4.00\,\mathrm{V}$). The 'harvested current' in Fig. 6 shows that the transfer window is clearly shifted to contain the peak of the primary current at its center. All the controls in Fig. 6 are working as intended, identical to Fig. 4. However, as mentioned earlier, the region 1 and 4 are barely visible as they are extremely brief compared to other phases.

The amount of energy harvested from a magnetic energy harvester using the TWA method increases as the core goes into deeper saturation. Fig. 7 illustrates such a behavior. In order to apply different levels of core saturation for the experiment, J is directly controlled by changing the level of the load voltage. Remember that the core goes into deeper saturation as J approaches to 0 since the transfer window is directly shrinking. A constant voltage source with a proper shunt impedance that can take in all the harvested current from the core is used as a replacement of supercapacitors. The level of the voltage source is varied from 0 V to 5.5 V. A current limited AC power source drives the primary side, with the current limited at $4.0\,\mathrm{A_{RMS}}$ (60 Hz). Using the AC power source is also benficial in generating a purer sine wave than the slightly distorted sine wave shown in Fig. 6 due to nonidealities coming from the load and the utility grid. The number of windings in the harvester core for Fig. 7 is $N = 200$. As the load voltage increases, the amount of power harvest also increases as predicted by our estimation. However, the gain in energy extraction by changing the load voltage (hence J) diminishes at higher voltage levels.

Fig. 8 illustrates an actual harvester prototype with all the circuit components of the test board neatly assembled in a tight space without testing terminals. The main bottlenecks for the size of the harvester are a magnetic core and supercapacitors. All other circuit components on the test board can be easily placed on top of the flat surface of the core. Considering that the circuit board of Fig. 8 also contains the initialization circuits and voltage regulation circuits that were not discussed in this paper, the actual size of an energy harvesting circuitry is even smaller than shown.

V. Remarks on Design Parameters

The required size of the core is directly related to the amount of harvested power as it changes A_{CORE} in (2). For example, a core with a wider cross-sectional area will have a longer transfer window, leading to a better power harvest overall. However, a smaller core clearly benefits in that it can be fitted into a much wider range of space constrained environments. Therefore, in conjunction with the level of the primary side current, the size of the core should be determined based on how much power is required by the circuit blocks that are connected as a load and how much space an installation requires.

For the TWA method, J ultimately determines the level of power harvest. Since J is proportional to N/V_{LOAD}, N and V_{LOAD} should be considered as a pair. First, N cannot be arbitrarily low because the thickness of the windings should be able to support the induced secondary current. Also, N should be sufficiently high so that $J \geq 0.314$ ($t_{\mathrm{SAT}} \geq \frac{T}{10}$) as discussed

earlier. On the other hand, a very high N makes construction of a core very difficult, and it also decreases an available window in the center of the core for the primary side wire (or forces a thinner wire for the same center window area). In our experiments, N from 200 to 500 was most useful with a wire gauge between AWG23 to AWG30. Second, V_{LOAD} can be as high as voltage ratings of supercapacitors allow. The problem is that voltage ratings of supercapacitors are usually a few volts, and J cannot be as minimized as desired. However, since $\sin(J)/J$ has a diminishing return as J approaches 0, it may be tolerable to select a slightly higher J. For example, V_{LOAD} of $4\,\mathrm{V}$ ($J = 0.8075$) can reach 91.06% of the power that V_{LOAD} of $10\,\mathrm{V}$ ($J = 0.3230$) harvests, assuming $N = 200$.

VI. Conclusion

This paper presents a new method to enhance energy extraction from magnetic energy harvesters. Compared to existing passive rectification as done in [6] and [7], the amount of harvested energy using the proposed TWA method is greatly improved. A test board and a prototype were constructed, and the improvement in the energy extraction using the TWA method was verified. The test result showed an example that improved the energy extraction by 70.73% from $38.6\,\mathrm{mW}$ to $65.9\,\mathrm{mW}$ at $J = 0.81$. The TWA method can be combined with active rectification without adding any physical complexity to the active rectification circuitry as well.

This paper has demonstrated that the energy extraction improves as a core goes into deeper saturation with the TWA method. This is different from conventional transformers or inductors where magnetic saturation is avoided. The level of magnetic saturation is also different from magnetic energy harvesters with passive rectification where a core is put into a soft saturation regime for the maximum energy extraction [6].

VII. Acknowledgment

The authors gratefully acknowledge the support of the Kwanjeong Educational Foundation, the Office of Naval Research Structural Acoustics Program, and The Grainger Foundation.

References

[1] J. Moon, J. Donnal, J. Paris, S. Leeb, "VAMPIRE: A magnetically self-powered sensor node capable of wireless transmission," *Applied Power Electronics Conference and Exposition (APEC), 2013 Twenty-Eighth Annual IEEE*, Mar. 2013.

[2] M. Minami, T. Morito, H. Morikawa, and T. Aoyama, "Solar biscuit: A battery-less wireless sensor network system for environmental monitoring applications." *The 2nd International Workshop on Networked Sensing Systems*, 2005.

[3] F. Simjee and P. Chou, "Everlast: Long-life, supercapacitor-operated wireless sensor node," *Proc. 2006 International Symposium on Low Power Electronics and Design. ACM*, pp. 197-202, 2006.

[4] S. Sudevalayam and P. Kulkarni, "Energy harvesting sensor nodes: survey and implications," *IEEE Commun. Surv. Tutorial*, vol. 13, no. 3, pp. 443-461, 2011.

[5] I. Stark, "Thermal energy harevsting with thermo life," *IEEE Intl. Workshop on Wearable and Implantable Body Sensor Networks*, pp. 19-22, Apr. 2006.

[6] J. Moon, S. Leeb, "Analysis model for magnetic energy harvesters," *IEEE Trans. Power Electron.*, vol 30, no. 8, pp. 4302-4311, Aug. 2015.

[7] J. Moon, S. Leeb, "Power flow control and regulation circuits for magnetic energy harvesters," *Control and Modeling for Power Electronics (COMPEL), 2014 IEEE 15th Workshop on*, pp. 1-8, Jun. 2014.

[8] S. Meninger, J. Mur-Miranda, R. Amirtharajah, A. Chandrakasan, and J. Lang, "Vibration-to-electric energy conversion," *IEEE Trans. Very Large Scale Integr. (VLSI) Syst.*, vol. 9, no. 1, pp. 64-76, Feb. 2001.

[9] G. Ottman, H. Hofmann, A. Bhatt, and G. Lesieutre, "Adaptive piezoelectric energy harvesting circuit for wireless remote power supply," *IEEE Trans. Power Electron.*, vol. 17, no. 5, pp. 669-676, Sep. 2002.

[10] I. Stark, "Thermal energy harevsting with thermo life," *IEEE Intl. Workshop on Wearable and Implantable Body Sensor Networks*, pp. 19-22, Apr. 2006.

[11] M. Pinuela, P. Mitcheson, S. Lucyszyn, "Ambient RF energy harvesting in urban and semi-urban environments," *IEEE Trans. Microwave Theory and Techniques*, vol. 61, no. 7, pp. 2715-2726, Jul. 2013